Air Pressure Differences over the Building Envelope: Case Studies

Lara Deprez[1], Kevin Verniers[*2], Ivan Pollet[2], Niek-Jan Bink[3], Jelle Laverge[1]

1 Ghent University, Department of Architecture and Urban Planning
Campus UFO T4, St-Pietersnieuwstraat 41
Ghent, Belgium

2 Renson NV
Maalbeekstraat 10
Waregem, Belgium
**Corresponding author: kevin.verniers@renson.be*

3 ACIN Instrumenten BV
Handelskade 76
Rijswijk, The Netherlands

ABSTRACT

Although the physics concerning air pressures in buildings don't differ between countries, often different reference values of the pressure difference over the envelope are used to determine air tightness and ventilation characteristics. The air transfer devices for natural ventilation, integrated in the façades or the internal building structure, are characterized at a pressure difference between 1 and 20 Pa depending on the country. For example, Belgium uses 2 or 10 Pa as a reference, the Netherlands adopts 1 Pa, whereas France applies 10 or 20 Pa. With respect to the building air tightness, the reference pressure used varies between 4 and 50 Pa over the countries.

To investigate this variability, differential air pressure measurements over the envelopes of two buildings were conducted within the context of a master's thesis. A Belgian single-family home and a high-rise student home were considered. The most elaborated case was the single-family home consisting of 2 floors and a flat roof where the following experiments took place. Firstly, the airtightness of the building envelope was determined based on three different test methods: a) the Blowerdoor test, b) the ACIN Air Tightness Tester or ATT, and c) the Pulse test. Secondly, simultaneous air pressure difference measurements were applied on all four walls of the home and at two different heights: floor and upper level. Lastly, wind speed sensors were attached in the middle of the exterior walls for measuring the wind speed near the wall surface. These measurements allowed (1) to compare the difference in measured building air tightness between the 3 test methods; (2) to analyse the variation of the pressure difference over the façades as a function of climate conditions; (3) to study the correlation between the local wind speed and the local pressure difference over the façade. For the high-rise building, only the measurements of air pressure difference and wind speed were conducted. These measurements were taken at the same façade at two different heights of the building. The results were compared with those found on the single-family house. An overview of the work done, used methodologies, and obtained results is presented in this paper.

KEYWORDS

Air pressure difference, air tightness, single-family home, high-rise building

1 INTRODUCTION

The air pressure difference across the building envelope is affected by indoor and outdoor air conditions that vary over time. This complicates the design of ventilation systems consisting of natural air transfer devices. Therefore, a reference value for the air pressure difference is adopted. However, countries do not necessarily use the same value. For example, Belgium uses 2 or 10 Pa (NBN, 1991; VEKA, 2021), the Netherlands adopt 1 Pa (NEN, 2001), whereas France considers 10 or 20 Pa (AFNOR, 2017; Effinergie, 2010).Next to this, an

effective ventilation system requires a good building air tightness, which is characterized also at a certain reference pressure. Again, there is no agreement on the used value, some countries adopt 4 Pa while others go up to 50 Pa (Buildwise, 2015).

A master's thesis was conducted due to diverse reference values. The paper includes: Section 2 detailing the measurements and buildings; Section 3 discussing differential pressure measurements and air tightness methods; and Section 4 summarizing the findings.

2 METHODOLOGY

2.1 Examined building types

Figure 1 presents two buildings: a two-storey single-family home and a 14-storey high-rise student home. The entire single-family home was accessible for the measurements. In contrast, the student home had only two available rooms on the 1st and 10th floors, both located on the same north-east oriented façade of the building. The single-family home has mechanical extract ventilation, which was at its lowest setting (about 35 m³/h) during the measurements. For the student home, only natural ventilation is available.

Figure 1: The single-family home (left) and the high-rise student home (right) considered in this study.

2.2 Measurement setup: building air tightness

The air tightness of the single-family home was assessed using the three methods listed below. All vents and windows were closed, but interior doors were left open. The ventilation system was turned off, except for the second method.

1. Blowerdoor test (BlowerDoor, 2024): This common test measures air tightness in units of 50 Pa. The home is subjected to both underpressure and overpressure conditions using a fan in an external door opening. The measurements are averaged to estimate the air leakage through the building envelope.

2. ACIN Air Tightness Tester or ATT (ACIN Instruments, 2024): This test uses an indoor located vessel with a differential pressure sensor. After the vessel is acclimatized, the ventilation system is turned on and off, and pressure variations in the vessel are monitored. After several cycles, the result is calculated and presented at the desired reference pressure.

3. Pulse test (Build test solutions, 2024): This test uses a small container filled with compressed air. One or more pulses are discharged to pressurize the building to 4 Pa. The building's air tightness is determined from the pressure drop and airflow measurements over time. This test is recognized in the UK.

2.3 Measurement setup: air pressure difference and wind sensors

The SDP810-125Pa (Sensirion, 2024) differential pressure sensor based on a thermal sensing element was used and located indoors. A flexible tube connected this sensor to a perforated sphere catching the wind. In addition, wind speed near the wall was measured using Adafruit's Anemometer (Adafruit, 2024), which can record wind speeds up to 70 m/s. The sensor data was collected using the Espressif ESP32-DevKitC (Espressif, 2024), which has Wi-Fi and Bluetooth. The data was sent to the Cloud and simultaneously saved on an SD card. To synchronize timestamps, each ESP32 device used the Network Time Protocol. A one-second sampling period was targeted due to the rapid changes of the wind.

In the single-family home, wall pressure differences were measured at the floor and upper levels of the four façades. Flexible tubes connecting the sensors to the corresponding perforated spheres ran through the trickle vents where they were present. All window vents were fully open. For the sake of consistency, the same tube length of 10 meters with an outside diameter of 6 mm was used for all measurements, since the properties of the tube affect the output of the sensor. Wind speed close to the wall was measured only at the floor level. Figure 2 shows part of the setup. Roof sensors measured wind speed and direction.

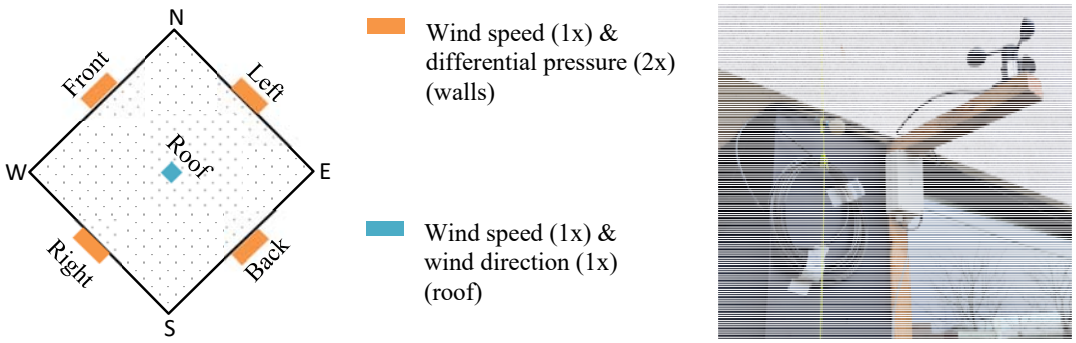

Figure 2: Left: sensor distribution in the single-family home (left). Right: illustration of the wind speed sensor and the perforated sphere (floor level) connected by a tube to a differential pressure sensor located indoors.

In the two rooms of the high-rise building, the same differential pressure sensor and wind speed sensor were mounted on a wooden plate in the window frame. The outer diameter of the tube remained unchanged, but the length was reduced to 0.5 meters. Figure 3 shows the setup on the 1st and 10th floors of the 14-story building.

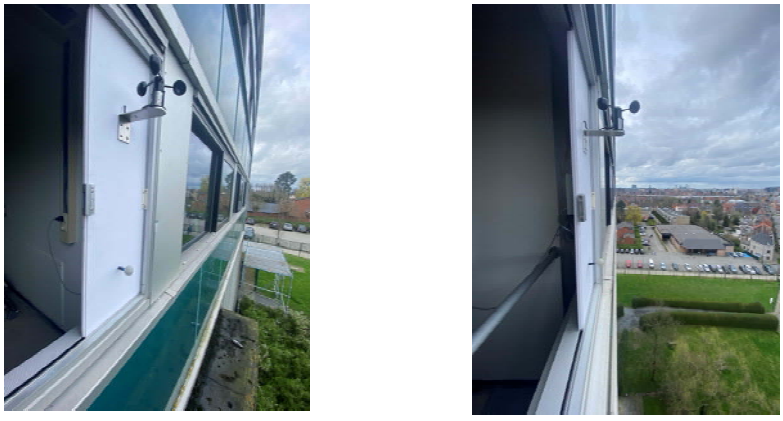

Figure 3: Measurement setup on the 1st (left) and 10th (right) floors of the high-rise building.

In this paper, overpressure is the case where the pressure across the outer wall is greater on the outside than on the inside, while underpressure represents the opposite.

3 RESULTS AND DISCUSSION

3.1 Air tightness measurements in the single-family home

Table 1 shows air leakage rates at both 50 and 4 Pa for the three air tightness methods under consideration, along with the corresponding n_{50} values. The converted air leakage rates, which are highlighted in italics, were derived using the Power Law for the Blowerdoor and ATT results. For the Pulse test, a specific formula was used to convert from 4 to 50 Pa (Build test solutions, 2021). Both the ATT and Pulse test were performed multiple times to check consistency between results.

The 2023 Blowerdoor test had a higher air leakage rate of about 35% compared to the 2019 test. The n_{50} value increased from 1.7 to 2.3 h^{-1}, possibly due to changes in the façades over past four years affecting its air tightness, as was also observed in other studies. The decreased flow exponent also reveals an increase of envelope cracks over time. The measured n_{50} value is a common value for new Flemish dwellings.

The ATT was combined with the house's mechanical extract ventilation system that depressurized the house. Measurements at the same location were nearly identical. Compared to the 2023 Blowerdoor test, the results of the ATT were similar or up to 12% higher when using the standard flow exponent of 0.66 of the ATT. When this exponent is adjusted to that of the Blowerdoor test, the ATT results were close to or about 10% lower than the Blowerdoor results (second rows for ATT in Table 1).

The Pulse test results at 50 Pa were higher, with deviations up to 30% compared to the 2023 Blowerdoor result. This could be due to the extrapolation formula used and potential inaccuracies from the used Pulse device that had already undergone several repairs.

For the 4 Pa results, similar deviations were observed between the Pulse and Blowerdoor tests. These deviations also occur compared to the ATT results, except that the ATT results were now barely higher than those of the Blowerdoor test.

Table 1: n_{50} and air leakage rates at 50 and 4 Pa for three air tightness test methods. Converted values in italics.

Air tightness test method	Flow exponent n	Air leakage rate [m³/h] 50 Pa	4 Pa	n_{50} [1/h]
Blowerdoor (under- & overpressure)				
2019: underpressure	0.690	965	*169*	1.6
2019: overpressure	0.780	978	*136*	1.7
2019: average	0.735	972	*153*	1.7
2023: underpressure	0.615	1314	*278*	2.2
2023: overpressure	0.671	1333	*245*	2.3
2023: average	0.643	1324	*262*	2.3
ATT (underpressure): 2023				
Test 1 downstairs: $q_{extract}$ = 326 m³/h; Δp=5.1 Pa	0.660	*1471*	*278*	2.5
	0.615	*1327*	*281*	2.3
Test 2 downstairs: $q_{extract}$ = 326 m³/h; Δp=5.2 Pa	0.660	*1452*	*274*	2.5
	0.615	*1311*	*277*	2.2
Test 3 upstairs: $q_{extract}$ = 326 m³/h; Δp=6.1 Pa	0.660	*1307*	*247*	2.2
	0.615	*1189*	*252*	2.0
Test 4 upstairs: $q_{extract}$ = 326 m³/h; Δp=6.0 Pa	0.660	*1321*	*249*	2.3
	0.615	*1201*	*254*	2.0
Pulse (overpressure): 2024				
Test 1: downstairs		*1450*	265	2.5
Test 2: downstairs		*1712*	317	2.9
Test 3: downstairs		*1676*	310	2.9

3.2 Differential pressure and wind speeds

The properties of the tube affect the readings of the differential pressure sensor (Sensirion, 2016). To calibrate, the output of the sensor was compared to a calibrated Setra Model 267, ranging from -100 to 100 Pa. Tube length in both cases was 0.5 or 10 meters, with a consistent outer diameter of 6 mm. Figure 4 shows a linear relationship in differential pressures between the sensors. The sensor used overestimates for 0.5 m and underestimates for 10 m. Regression line equations from Figure 4 are used to correct this. The 10 m equation is used for the single-family home, and the 0.5 m equation for the high-rise student home.

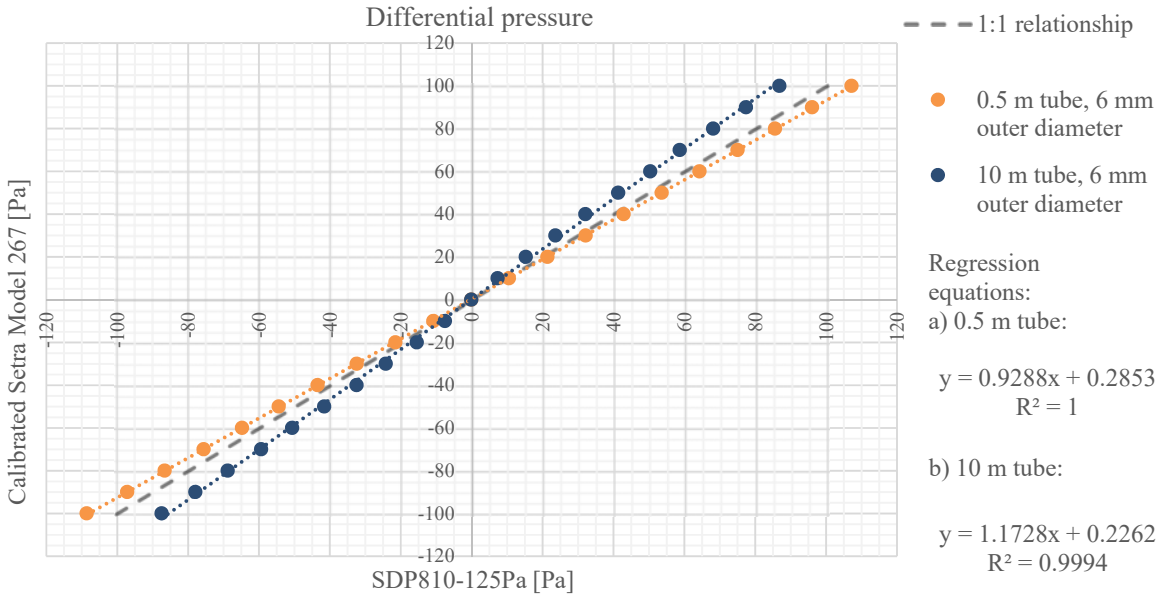

Figure 4: Relationship between a Setra Model 267 and a SDP810-125Pa with a 6 mm tube of 0.5 or 10 m length.

From January 17 to February 9, 2024, measurements were taken in the single-family home, and from March 7 to April 10, 2024, in the high-rise building. The time distribution between over- and underpressure conditions at each point is shown in Figure 5. In the high-rise building, the 1st floor façade experienced overpressure 90% of the time, dropping to nearly 50% on the 10th floor. The façade was mainly exposed to the leeward side, so the underpressure at the top was higher. Also the stack effect will slightly contribute. A similar trend was observed in the single-family home with the mechanical extract ventilation operating at 10% of its nominal rate (about 35 m³/h), with the upper level being in overpressure for less time than the floor level. Pressure varied between the façades due to wind effects. The south-west and south-east walls had predominantly positive pressure differences. In contrast, on the north-east and north-west upper levels, the pressure differences were mostly negative.

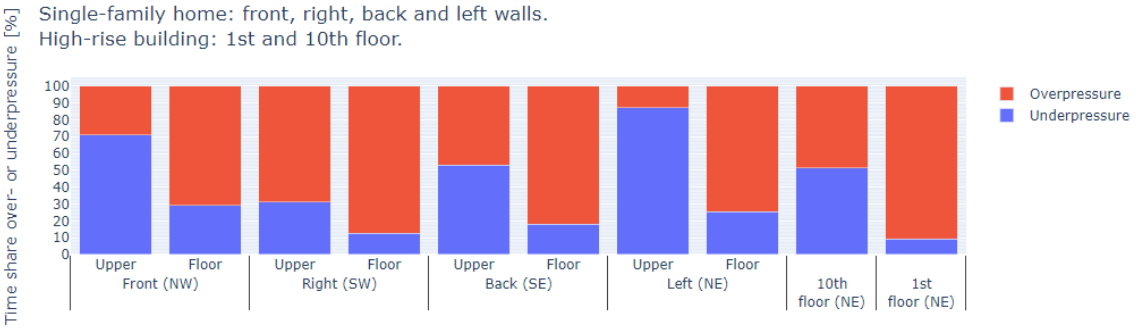

Figure 5:Time distribution between over- and underpressure conditions at each measurement point.

Figure 6 shows the Cumulative Distribution Functions (CDFs) of all pressure differences. The top graph illustrates the overpressure CDFs, while the bottom graph presents the absolute underpressure CDFs of both buildings.

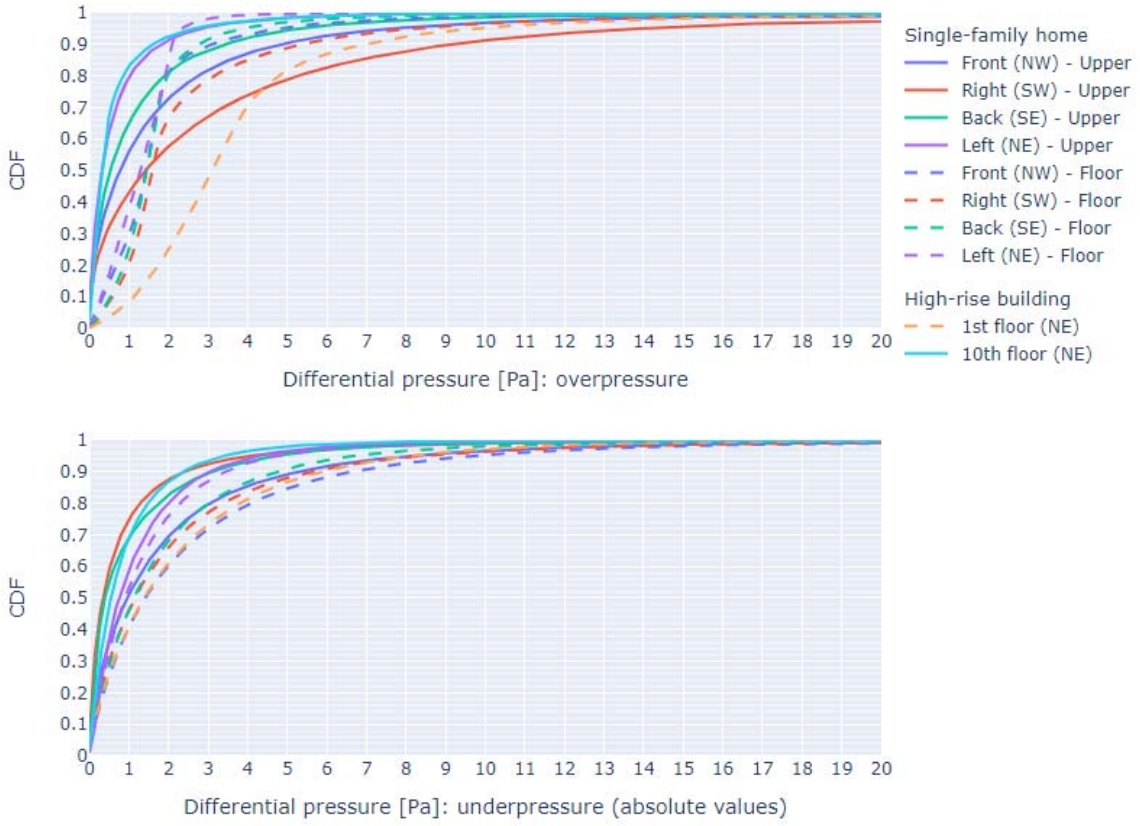

Figure 6: Cumulative distribution functions (CDFs) of the pressure differences across the façades of the single-family home and the high-rise building.

For the high-rise building, the overpressure CDF rises clearly faster at low pressure on the 10th floor than the 1st. Moreover, the 1st floor's CDF has an S-shape and is shifted to the right, illustrating the high positive pressure offset at the bottom of the façade, due to wind and stack effects. The P50 values are 0.3 and 3.1 Pa for the 10th and 1st floors, respectively. The underpressure CDF for 10th floor is again steeper than the 1st's. Unlike overpressure CDFs, the 10th floors increase is less distinct, while the 1st floor's increase is more pronounced but without S-shape. The P50 values for underpressure are 0.5 and 1.4 Pa for the 10th and 1st floors, respectively.

For the single-family home, the overpressure CDFs at pressures below 1 Pa rise clearly slower at the floor level than the upper levels, likely due to the stack effect and wind effects. Between 1 and 2 Pa, the upper level's CDFs fall below the floor levels', possibly due to wind effects. At floor level, also an S-shape was observed in the overpressure CDF at all façades. The south-west wall shows the slowest increase in both levels, indicating higher overpressures. As a consequence, the opposite north-east façade experienced the lowest overpressures. The P50 values for the south-west wall are 1.4 and 1.6 Pa for the upper and floor levels, respectively, while its 0.3 and 1.3 Pa for the north-east wall.

The underpressure CDFs for the single-family home reveal that the floor level values surpass the upper levels. Examining the façades, the north-west has the least increase at both levels,

with P50 values of 1.4 and 1 Pa. The north-east wall shows a moderate and similar increase at the upper level and the floor level, with P50 values of 0.8 and 0.9 Pa. The south-east wall has the second-highest increase at both levels, with P50 values of 0.3 and 1.1 Pa. The south-west wall exhibits the highest increase at the upper level but a moderate rise at the floor level, with P50 values of 0.4 and 1.2 Pa. These variations could be due to wind effects.

Figure 7 shows the relationship between wind speeds near the walls and façade pressure differences, represented by boxplots for both over- and underpressure. The wind speeds are categorized according to the Beaufort scale.

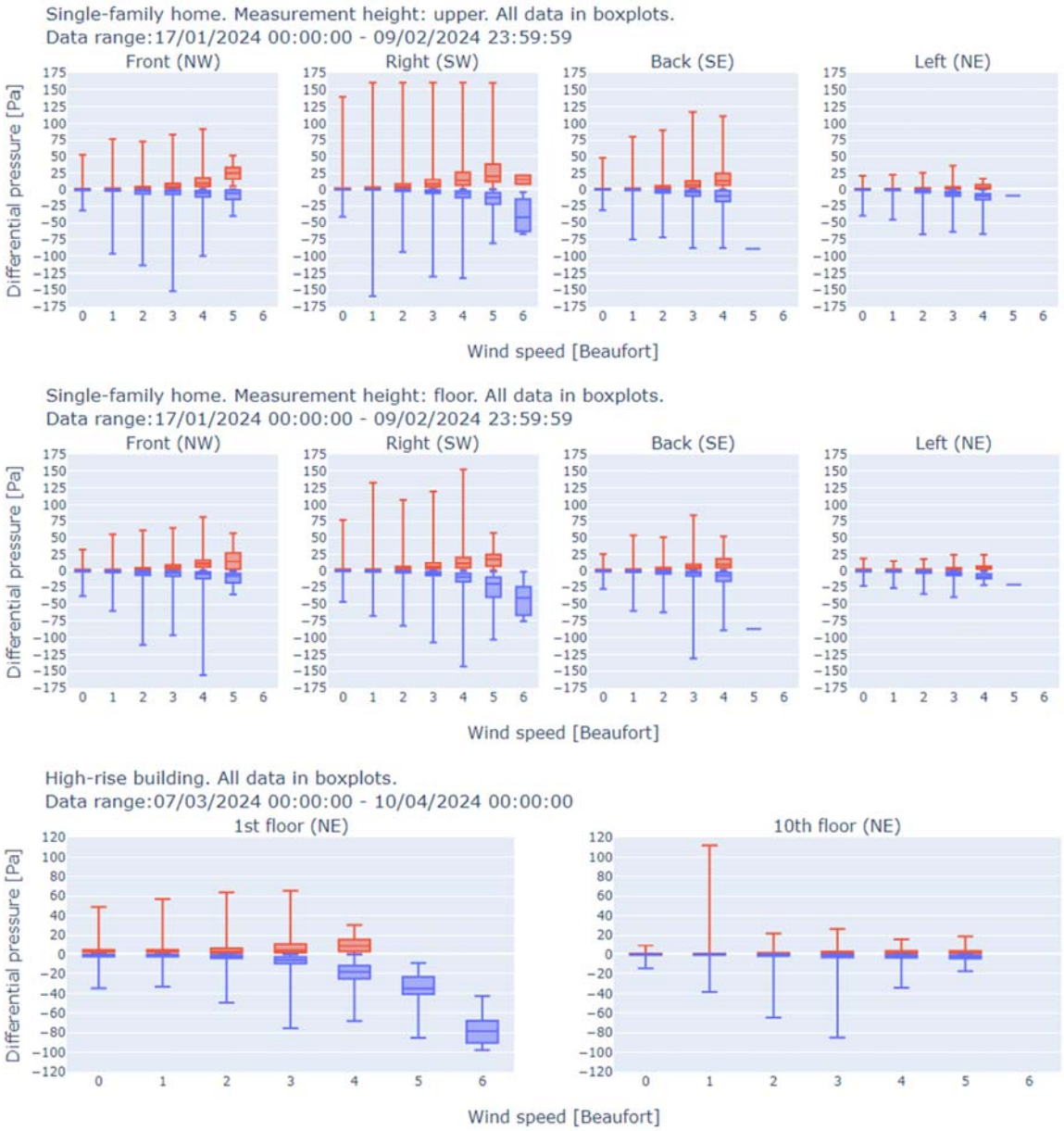

Figure 7: Boxplots of positive and negative median differential pressures as a function of median wind speed, classified by the Beaufort scale. All data points included in boxplots.

The boxplots reveal a substantial variation in differential pressure regardless of wind speed, especially on the south-west wall of the single-family home. As the wind speed escalates, the absolute value of the median increases. Theoretically, this increase should be according to the

square of the wind speed. This is demonstrated in Figure 8 where the median wind speed and median differential pressure for Beaufort classes 0 through 4 from Figure 7 were chosen and fitted using the formula ax^2+b. The coefficients of determination (R^2) are generally above 0.9, with only 2 of 16 cases falling below R^2 of 0.9 due to minor pressure differences between the Beaufort classes under consideration. The pressure difference seems to quite well predict the local wind speed, if the quadratic relation is known. Figure 7 shows that pressure differences across the wall, even when the vent is open, can sporadically escalate to substantial levels. This underscores the necessity of employing pressure-regulated vents. Generally speaking, the measured pressure differences are rather low: approximately 50% of the values are less than +1 Pa and 90% of the values range from 2 to 10 Pa, excluding any negative values.

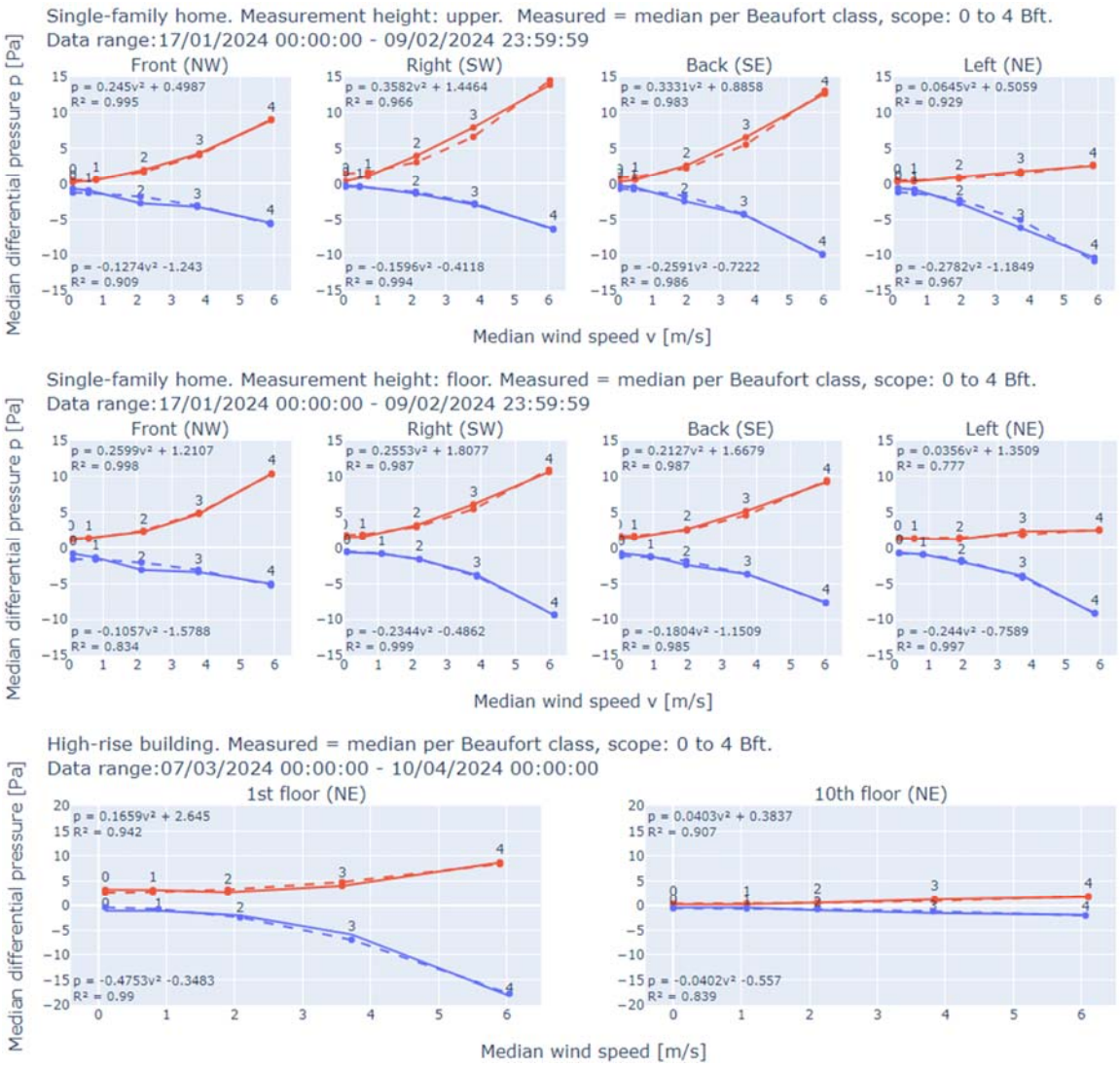

Figure 8: Median differential pressure as a function of median wind speed for Beaufort classes 0 through 4. Measured values derived from Figure 7. Curve fitting is employed to highlight quadratic correlation between wind speed and differential pressure.

Figure 9 shows the CDFs of the infiltration and exfiltration air leaks, where infiltration represents the case overpressure and exfiltration the case underpressure. The curves are obtained as follows. Each measured pressure difference is converted to its corresponding flow rate using the Power Law. The flow coefficient and exponent are derived from the Blowerdoor 2023 test. If the measured pressure is positive, the overpressure result from the

Blowerdoor test is used. For a negative pressure, the underpressure parameters are adopted. For conversion to flow, the flow coefficient is divided by eight because there are eight measurement locations around the house, while all walls have an equal area and it is assumed that the leaks are evenly distributed while an airtight roof is taken into account. Finally, for each time instant, the positive flow rates are added together and the same is done for the negative flow rates. This results in two time series representing overpressure and underpressure from which their CDFs are obtained.

The exfiltration CDF rises at lower flow rates compared to the infiltration CDF. This is due to the mechanical extract ventilation system operating at its minimum level, which is about 35 m³/h, during the measurements. At P50, the air leakage rates for exfiltration and infiltration are 36 and 71 m³/h, respectively. The difference between these two rates approximates the minimum airflow rate of the ventilation system. At P90, both infiltration and exfiltration increases to about 120 m³/h.

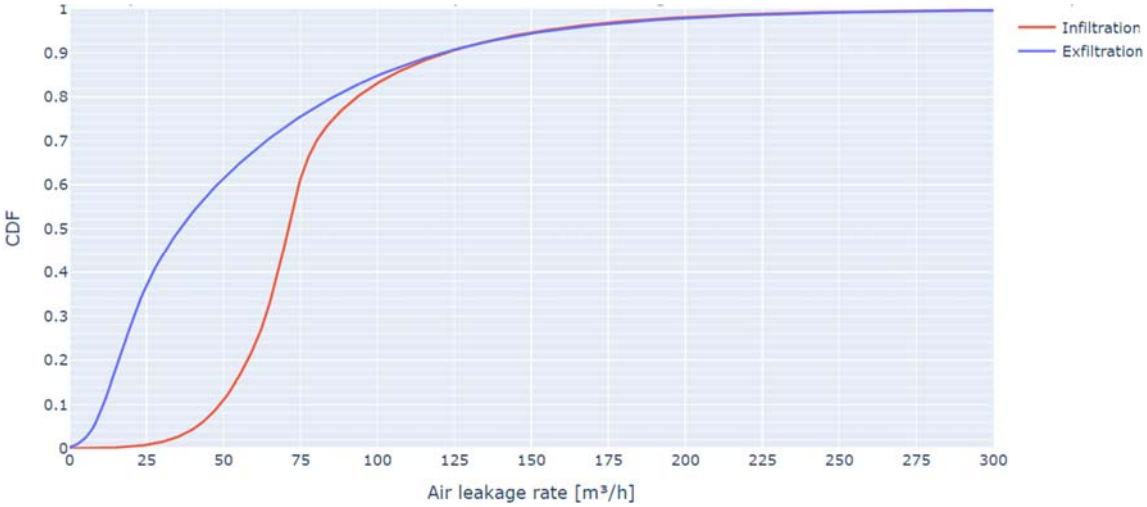

Figure 9: Single-family home: cumulative distribution functions of in- and exfiltration.

4 CONCLUSIONS

The air tightness measurements in the single-family home show, for a reference pressure of 50 Pa, that the ATT results are comparable to, if not marginally higher than, the Blowerdoor test. When the reference pressure is changed to 4 Pa, the ATT gives similar or slightly lower values than the Blowerdoor test. When the flow exponent in the ATT's calculation is set equal to that of the Blowerdoor test, the results of the ATT are marginally lower for both 50 and 4 Pa. In contrast, the Pulse test gives persistently higher results than the Blowerdoor (up to 30%), regardless of the 50 or 4 Pa reference pressures.

The cumulative distribution functions of the pressure differences show that the wind effect is prominent for both types of buildings, highlighting the need for pressure-regulated vents. The contribution of the stack effect can also be observed between measurements at different heights. For the high-rise building, the median overpressures at P50 are 3.1 and 0.3 Pa for the 1st and 10th floors, respectively, while underpressure values are 1.4 and 0.5 Pa. For the single-family home, the wind effect is clearly noticeable, with the south-west façade frequently experiencing overpressure. The P50 values for all façades fall within the range of -1.5 to 1.5 Pa.

A high correlation ($R^2 > 0.9$) between the square of the local wind speed and the differential pressure is found at most measuring points of both buildings, expressed as a quadratic

relationship between the median values. However, this relationship shows marked variability between façades, depending on the wind effect. At a Beaufort scale of 2, both buildings showed median pressure differences ranging from about 3 to -3 Pa. As the Beaufort scale increased to 4, the range broadened from 8 to -6 Pa. This effect is less visible on the 10th floor of the high-rise building because the both positive and negative median pressures remained low at 2 and -2 Pa, respectively.

The cumulative distribution functions of the infiltration and exfiltration leakage rates of the single-family home show the effect of the mechanical extract ventilation system. The exfiltration curve increases at lower leakage rates compared to the infiltration curve. At P50, the infiltration rate is 71 m³/h, while the exfiltration rate is 36 m³/h. The difference between these two rates is equal to the minimum airflow at which the mechanical extract ventilation system operated during the measurements.

5 REFERENCES

ACIN Instruments. (2024). *Air Tightness Tester*. Retrieved from https://acin.nl/en/air-tightness/air-tightness-tester/

Adafruit. (2024). *Anemometer wind speed sensor*. Retrieved from https://www.adafruit.com/product/1733

AFNOR. (2017). NF DTU 68.3:2017. *Travaux de bâtiment - Installations de ventilation mécanique*. French Standardization Association.

BlowerDoor. (2024). *BlowerDoor Measuring Principle*. Retrieved from https://www.blowerdoor.com/measurement-systems/blowerdoor-standard/the-measuring-principle

Build test solutions. (2021). Retrieved from https://www.buildtestsolutions.com/files/9705531c5d8042ce38699e0e934e51332879eb24.pdf

Build test solutions. (2024). *Measuring building air tightness with Pulse*. Retrieved from https://www.buildtestsolutions.com/air-leakage-testing/pulse-air-permeability-testing/how-it-works

Buildwise. (2015). *TV255: Luchtdichtheid van gebouwen.* Buildwise. Retrieved from https://www.buildwise.be/nl/publicaties/technische-voorlichtingen/255/

Effinergie. (2010). Guide de la ventilation naturelle et hybride "VHNY".

Espressif. (2024). *ESP32-DevKitC*. Retrieved from https://www.espressif.com/en/products/devkits/esp32-devkitc/overview

NBN. (1991). NBN D50-001:1991. *Ventilation systems for housings*. Belgian Bureau for Standardization.

NEN. (2001). NEN1087:2001. *Ventilation in buildings - Determination methods for new estate*. Netherlands Standardization Institute.

Sensirion. (2016). *Compensation of pressure drop in a hose*. Retrieved from https://sensirion.com/media/documents/E2B13D4F/6166C422/Sensirion_Differential_Pressure_Datasheet_SDP800_Pressure_drop_in_ho.pdf

Sensirion. (2024). *SDP810-125Pa*. Retrieved from https://www.sensirion.com/products/catalog/SDP810-125Pa

VEKA. (2021). Bijlage IX - ventilatievoorzieningen in woongebouwen: bepalingsmethode en eisen.